# POLITECNICO DI TORINO
## Repository ISTITUZIONALE

Loss-of-heat-sink transient simulation with RELAP5/Mod3.3 code for the ATHENA facility

(Article begins on next page)

22 December 2024
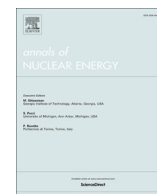
# Loss-of-heat-sink transient simulation with RELAP5/Mod3.3 code for the ATHENA facility

T. Del Moro [a,*], F. Giannetti [a], P. Cioli Puviani [b], I. Di Piazza [c], D. Diamanti [c], M. Tarantino [c]

[a] *Sapienza University of Rome, Corso Vittorio Emanuele II, 244, 00186 Rome, Italy*
[b] *Politecnico di Torino, Corso Duca degli Abruzzi, 24, 10129 Torino, Italy*
[c] *ENEA, Brasimone, 40032 Camugnano, Bologna, Italy*

## ARTICLE INFO

## ABSTRACT

ATHENA (Advanced Thermal-Hydraulic Experiment for Nuclear Applications) is a large multipurpose pool-type lead-cooled facility under construction at the Mioveni site in Romania. It has been identified by the FALCON (Fostering ALfred CONstruction) Consortium to characterize large to full-scale ALFRED components, to conduct integral tests, and to investigate the main thermal–hydraulic phenomena inherent in pool-type systems. ATHENA is representative of ALFRED in terms of the difference in height of the thermal barycenters of the heat source and heat sink, i.e., 3.3 m, in order to reproduce the buoyancy forces in the system. Similar to ALFRED's design, ATHENA minimizes thermal stratification within the main vessel even under natural circulation conditions, through an internal structure referred to as "barrel". This structure directs the fluid flow towards the main vessel, preventing fluid stagnation near the vessel itself. The paper initially provides a steady-state thermal–hydraulic characterization of the facility, including details of the numerical model developed using the RELAP5/Mod3.3 thermal–hydraulic code. Then, focus is given to the transient analysis considering as a reference scenario a Loss-of-Heat-Sink (LOHS) accidental transient. In this scenario, the Main Circulation Pump (MCP) is assumed to remain operational while the Core Simulator (CS) is deactivated once the lead temperature at the Main Heat Exchanger (MHX) outlet reaches a predefined threshold. A sensitivity analysis is conducted with set points of 430 °C, 450 °C, 470 °C, and 490 °C, assessing the system's response following MHX isolation from the secondary loop. The study evaluates the impact of different CS deactivation set points on reactor SCRAM delay (reducing CS power to a level representative of decay heat) as well as on system maximum and minimum temperatures.

## 1. Introduction

Within the context of the R&D program for the advancement of Generation IV (Gen IV International Forum; Lorusso et al., 2018) Nuclear Power Plants, the Heavy Liquid Metal Fast Reactors (HLMFRs) (Tarantino et al., 2021) emerge as highly promising technologies capable of meeting the safety and reliability standards required for the civil nuclear power applications. Among the various technologies chosen by the Generation IV International Forum (GIF), Lead-cooled Fast

Reactors (LFRs) hold a prominent position due to their advanced stage of development. ALFRED (Advanced Lead Fast Reactor European Demonstrator) (Alemberti et al., 2015; Frignani et al., 2017; Frignani et al., 2019) has been selected by the FALCON Consortium as the current design to showcase the LFR technology. ALFRED will be constructed at the Mioveni site (Romania), together with additional facilities belonging to the ALFRED Research Infrastructure (RI) (Constantin et al., 2021) designed to support the reactor development.

ATHENA (Advanced Thermal-Hydraulic Experiment for Nuclear

---

\* Corresponding author.
*E-mail addresses:* tommaso.delmoro@uniroma1.it (T. Del Moro), fabio.giannetti@uniroma1.it (F. Giannetti), pietro.ciolipuviani@polito.it (P. Cioli Puviani), ivan. dipiazza@enea.it (I. Di Piazza), dario.diamanti@enea.it (D. Diamanti), mariano.tarantino@enea.it (M. Tarantino).

Applications) (Del Moro et al., 2022) will be the largest lead-cooled pool-type facility in Europe, aimed at evaluating the thermal-–hydraulic behavior of 1:1 scaled ALFRED components, as well as at assessing the performance of the coolant chemistry control system within a large pool environment. While ATHENA's primary focus is to test mainly the Core Simulator (CS, detailed in Section 2.2) (Cioli Puviani et al., 2023) and the Main Circulation Pump (MCP) under steady-state conditions, it will be also used to conduct selected accidental transients to evaluate the system's response to Postulated Initiating Events (PIEs), and to compare experimental to numerical simulation results.

This paper focuses on a specific PIE: the isolation of the heat sink, i.e., the Main Heat eXchanger (MHX) (Del Moro et al., 2022; Del Moro et al., 2023), achieved by closing the interception valves on the secondary side of the MHX, resulting in a Loss-Of-Heat-Sink (LOHS) transient. The decrease in the cooling power of the MHX causes an increase in the lead temperature, triggering the SCRAM once a predefined set point value is reached. The subsequent analysis serves as a pre-test analysis for a future experimental run on the facility. The code used to simulate the thermal–hydraulic behavior of the facility is RELAP5/Mod3.3 (Information System Laboratories, 2003) with the implementation of the HLM thermo-physical properties.

After a brief description of the ATHENA facility, Section 4.1 provides details on the numerical model and the steady state conditions achieved before the transient. Then, Section 4.2 outlines the boundary conditions for executing the transient and discusses the results. In Section 4.3, a sensitivity analysis on the selected set point is conducted, providing a discussion on the results.

## 2. ATHENA: A step towards ALFRED reactor

### 2.1. ALFRED and ALFRED research infrastructure

ALFRED, in its revised configuration, will be the European Demonstrator of the LFR technology. Its design is carried out by the FALCON Consortium, composed of ENEA (Italy), Ansaldo Nucleare (Italy), and RATEN ICN (Romania). ALFRED is a 300 MWth pool-type reactor, with all the components removable, and using proven and already available technology. The main advantage of this characteristic is the possibility to conduct the in-service inspection, that would otherwise not be possible in a lead environment. Great attention has been paid to the natural circulation, thus selecting components design and flow path in such a way to minimize the pressure drops.

The lead exits the core and it is moved by the Primary Pump (PP) towards the Steam Generator (SG), where it flows downward and in countercurrent with respect to the secondary water/steam mixture. Then, it goes into the cold pool, and enters the core again. Two regions can be distinguished in ALFRED: the hot pool, that is located between the PP and the SG, and the cold pool, which occupies most of the Reactor Vessel (RV) volume, in such a way to reduce the average temperature in cases in which the heat sink is not available in some accidental transients. The Decay Heat Removal system (DHR) is composed of two passive, redundant and independent system, each one composed of four Isolation Condensers (ICs) connected to the secondary side of four SG.

The construction is planned at the Mioveni site, in Romania, along with the related RI. The RI comprehends six experimental facilities, each of them focusing on a particular aspect of the LFRs to be investigated. The facilities are:

- ATHENA, that will be better described in Sect. 2.2, and it focuses on (i) the main TH phenomena involved in a LFR pool-type reactor, i.e., lead flow inside the Fuel Assembly (FA), pool mixing, (ii) components testing at relevant scales for ALFRED, and (iii) oxygen control system verification.

- ChemLab: it is a laboratory for the study of the coolant chemistry and its interaction with the structural materials. It will be composed of an experimental section and a metallographic laboratory.
- HELENA2: it will be a loop-type facility for FA TH characterization, Flow Induced Vibration (FIV) experimental analysis, and control rods testing.
- ELF: it will be a large scale pool-type facility for long term experiments and components testing at relevant scale for ALFRED reactor, both under forced and natural circulation. It will be composed of a 10 MW CS, four SGs, two PPs, and the DHR.
- Hands'ON: it will be a pool-type facility aimed at simulating the fuel handling procedures and components.
- Meltin'Pot: it is composed of four modules, focused on (i) the fuel–coolant interaction, (ii) fuel dispersion/relocation, (iii) fission products dispersion/retention in lead and/or migration in cover gas, and (iv) polonium retention/dispersion in lead, respectively. This facility will contain radioactive material, and thus it will be hosted in a Hot Cell.

### 2.2. ATHENA experimental facility

ATHENA (Advanced Thermo-Hydraulics Experiment for Nuclear Application) is a multipurpose experimental facility, designed to conduct experiments representative of ALFRED operation. Its capabilities encompass a wide array of investigations related to LFR technologies. For instance, ATHENA allows study on pool thermal-hydraulics, heat transfer through the InterWrapper (IW) region in a multi-assemblies core, the heat exchanger behavior, and the MCP performance assessment under both normal and transient conditions. Moreover, ATHENA provides a platform for safety-related tests; such as simulating the heat exchanger tube rupture or the fuel assembly (FA) partial blockage. ATHENA can provide a large data base of experimental data for the code validation, perform R&D investigations related to the lead technology, test components in full scale.

ATHENA is a pool type facility, where the components of the primary system are installed in a large vessel, having an internal diameter of 3.2 m and a height of about 10 m. The main parameters that characterize ATHENA facility are reported in Table 1, while Fig. 1 shows pictures of the Main Vessel and the lead Transfer Tank.

#### 2.2.1. Primary system

The primary system is coupled to a secondary system via the MHX, utilizing pressurized water. Inside the main vessel (see Fig. 2), an internal vessel, named barrel, is situated. Its purpose is to promote the lead flow within the pool, ensuring sufficient mixing and a uniform thermal profile in the cold pool. Cold lead enters the CS from through the feeding duct from the bottom of the main vessel. The CS includes 126 electrically heated pins, and one central dummy, with the diameter and pitch of the fuel pins based on those of the ALFRED reactor. The 126 pins are included inside a central hexagonal assembly and 6 peripherals trapezoidal assemblies. This layout allows to perform investigations on the

**Table 1**
ATHENA main parameters.

| Parameter | Unit | Value |
|---|---|---|
| Main Vessel diameter | m | 3.2 |
| Main Vessel height | m | 10.0 |
| Power | MW | 2.21 |
| Number of pins in the Core Simulator | – | 126 + 1 (dummy) |
| Pin bundle pitch-to-diameter ratio | – | 1.29 |
| Core Simulator Active length | mm | 810 |
| Main Circulation Pump head | bar | 2.0 |
| Main Heat Exchanger tubes number | – | 91 |
| Tube bundle pitch-to-diameter ratio | – | 1.3 |
| Main Heat Exchanger tubes active length | m | 3.0 |
| Lead temperatures | °C | 400–520 |
| Maximum lead flow rate | kg/s | 189 |

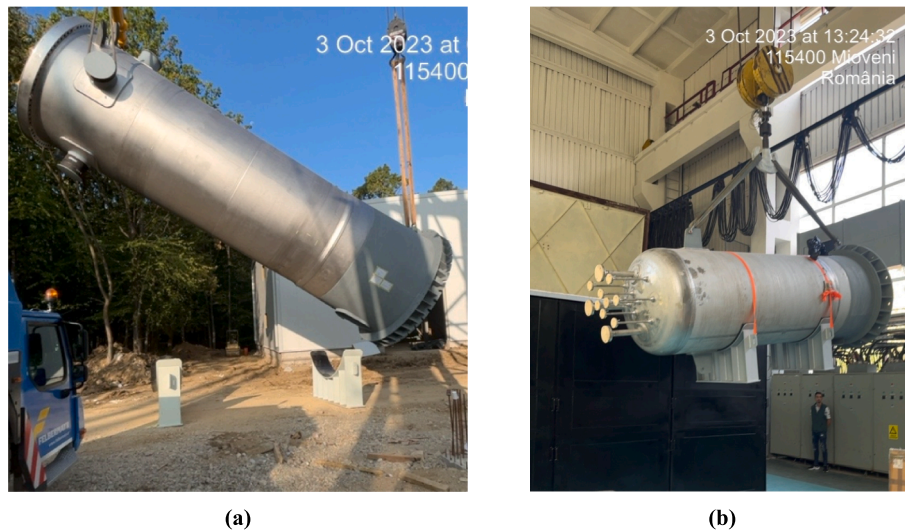(a)                                           (b)

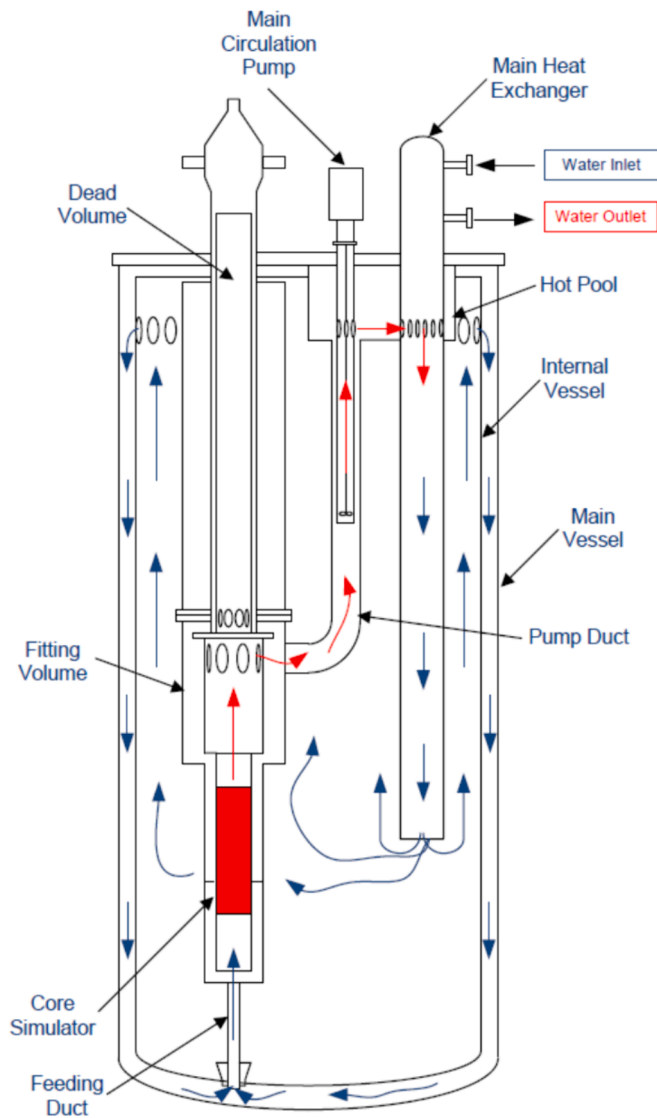**Fig. 1.** Pictures of the ATHENA Main Vessel (a) and the Transfer Tank (b).



**Fig. 2.** ATHENA primary system – Schematic drawing.

lead flow and the heat transfer inside the central assembly, while the six external assemblies have the scope to provide the correct boundary conditions for the central one. The total power of the CS is 2.21 MW, representative of an average ALFRED FA (Grasso et al., 2014). Fig. 3 depicts a schematics of the CS.

The lead temperature is 400 °C at the inlet of the CS and 480 °C at the exit, in accordance with the lead thermal cycle foreseen for the Stage 2 of ALFRED operation; furthermore, it is also possible to reach a maximum temperature of 520 °C, in agreement with the Stage 3 of ALFRED operation. The heated lead exits from the CS and enters in the hot pool, passing through the fitting volume and the pump duct. The main circulating pump, which pushes the lead, is vertical, axial type. From the hot pool, the lead enters inside the MHX, which is bayonet tube type, with three concentric tubes (see Fig. 5 and Fig. 6). At the exit of the heat exchanger, the lead temperature is about 400 °C; then it rises along the internal pool and goes down through the annular space between the main vessel and the internal vessel, to enter again in the CS from the
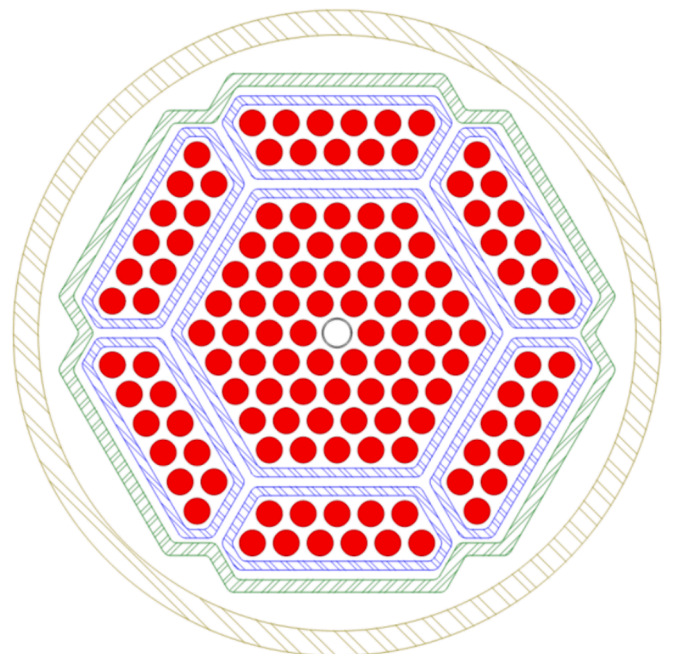


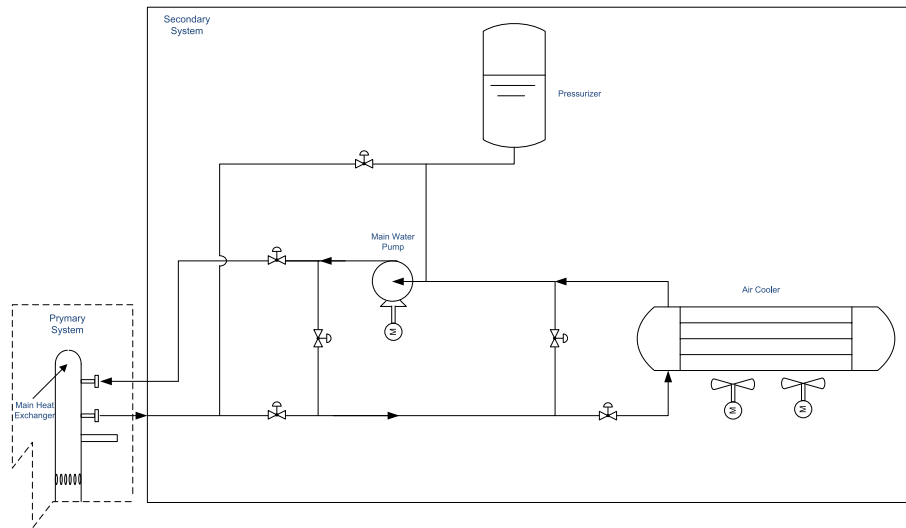**Fig. 3.** Schematic layout of ATHENA core simulator.
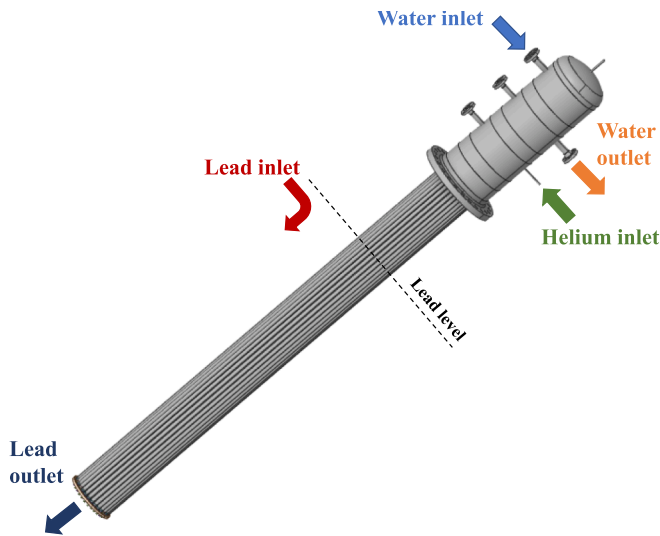
Fig. 4. ATHENA secondary system – Schematic drawing.
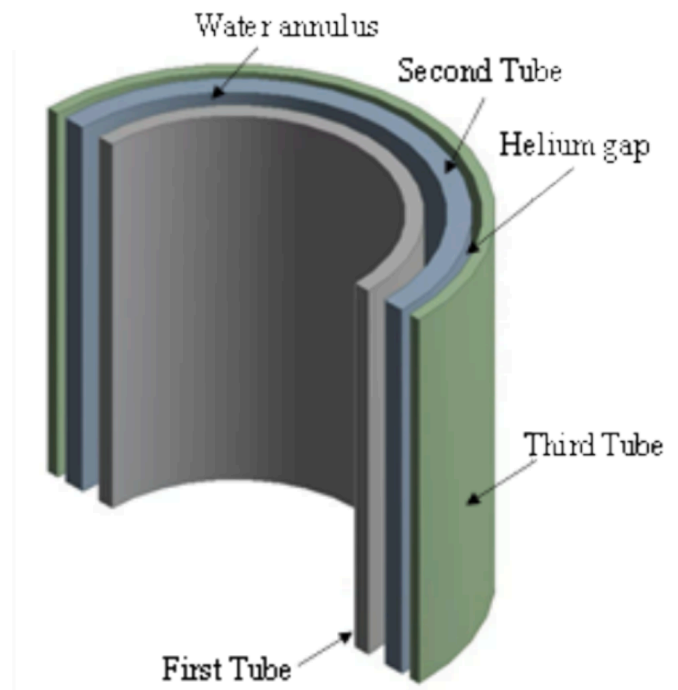


Fig. 5. ATHENA Main Heat Exchanger.

bottom of the main vessel.

### 2.2.2. Secondary system

Fig. 4 illustrates a schematic representation of the secondary system of ATHENA. It is mainly composed of a pressurizer (PRZ), an air cooler (AC), and a main water pump (PC). The heat is extracted from the primary system by the bayonet tubes type MHX, and it is eventually dissipated into the environment by the AC. The thermal power to be removed is 2.21 MW. The fluid circulating in the secondary system is demineralized water, pressurized by a nitrogen cover gas in the PRZ. The working conditions of the secondary system are resumed in Table 2. For the purposes of this paper, only conditions corresponding to Stage 3 have been considered.

## 3. RELAP5 Numerical Model

The numerical model of ATHENA facility has been realized by the System Thermal-Hydraulic (STH) code RELAP5/Mod3.3, in which the thermo-physical properties of HLMs have been implemented (Oriolo et al. 2000; Martelli et al., 2019). The fluid domain of the facility (lead, water, and air sides) is simulated using pipes, branches, and single



Fig. 6. Bayonet tube detail of the ATHENA Main Heat Exchanger.

**Table 2**
ATHENA secondary system – Working conditions.

| Parameter | Stage 2 | Stage 3 |
|---|---|---|
| Inlet lead temperature (°C) | 480 | 520 |
| Outlet lead temperature (°C) | 400 | 400 |
| Water pressure (MPa) | 1.2 | 2.5 |
| Inlet water temperature (°C) | 110 | 110 |
| Outlet water temperature (°C) | 160 | 200 |

junctions. Heat structures are used to simulate the metallic and insulating structures. Pumps and valves have been modeled though the corresponding RELAP5 components and are used to provide the nominal mass flow rates regulated by suitable control systems. Time dependent volumes and time dependent junctions serve as boundary conditions,

controlling parameters such as cover gas pressure, pressurizer pressure, and air mass flow rate in the AC. Boundary conditions for convective heat transfer towards the environment are provided though a constant heat transfer coefficient equal to 8 W/m$^2$ K, and a constant external temperature equal to 10 °C.

The nodalization strategy employed for the entire lead domain, including the MHX immersed in the lead, adopts the so-called "sliced modeling approach" (Narcisi et al., 2019). This method consists of discretizing with the same axial dimension all the fluid elements at the same absolute height. In such a way, phenomena such as natural circulation can be better reproduced by the code. The average length of the control volumes in the pool ("3D" region) is about 30 cm, since large fluid volumes require large axial length of the cell to meet the typical criterion for STH codes of L/D > 1 (Information System Laboratories), whereas a mesh sensitivity analysis has been carried out in the "1D" active regions where the hydraulic diameter is much smaller, i.e., CS and MHX, starting from a reference average length of ~15 cm and doubling or halving such value. Results of such analysis are reported in Fig. 7 and Fig. 8, where the convergence to a steady state value is achieved regardless of the cell size in the active regions. In the figures, the x-axes contain the component where the mesh size has been refined or enlarged ("CS" or "MHX") and a number that indicate if the mesh is finer or coarser ("1" for refined, "2" for coarser) with respect to the reference mesh. In particular, Fig. 7 shows that the mass flow rate distribution among the FAs is the same in the three tested cases, while Fig. 8 shows a greater impact of the nodalization in the MHX. Nevertheless, it still does not significantly impact on the results, being the maximum discrepancy on the lead temperature difference across the MHX of ~0.4 °C, that in terms of exchanged power corresponds to 0.4 %. However, an intermediate size of the cell of ~15 cm has been selected in both the components to achieve a higher level of detail in the components themselves, allowing to obtain at the same time a homogeneous mesh in the system. In such a way, each fluid element in the pool corresponds to 2 fluid elements in the active regions. Fig. 9 illustrates the axial nodalization solely of the "1D" region, representing the path from the feeding conduit to the MHX. It is worth noting that the CS is modeled by three parallel pipes, each one representing the central hexagonal FA, the trapezoidal FAs, and the bypass or IW region, respectively.

The pool side of the ATHENA main vessel has been further azimuthally discretized into 3x120° sectors. The division into three sectors should in principle allow to represent eventual recirculation and fluid mixing in large pool domains. By adopting the same azimuthal angle for each sector, almost the same cross-sectional areas are achieved, mitigating numerical oscillations in the results. As shown in
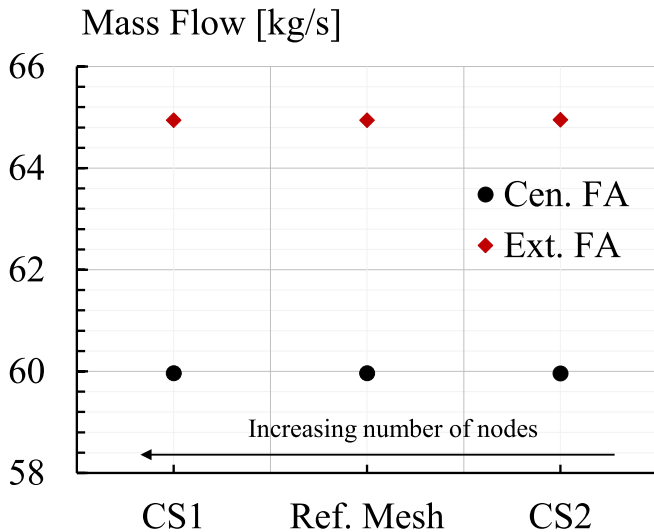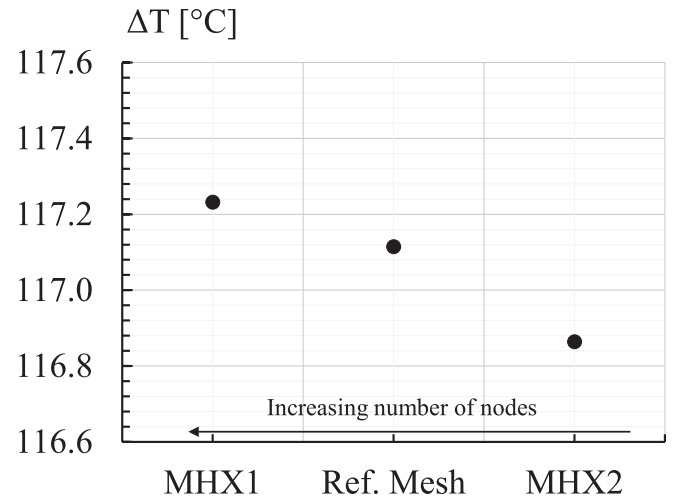


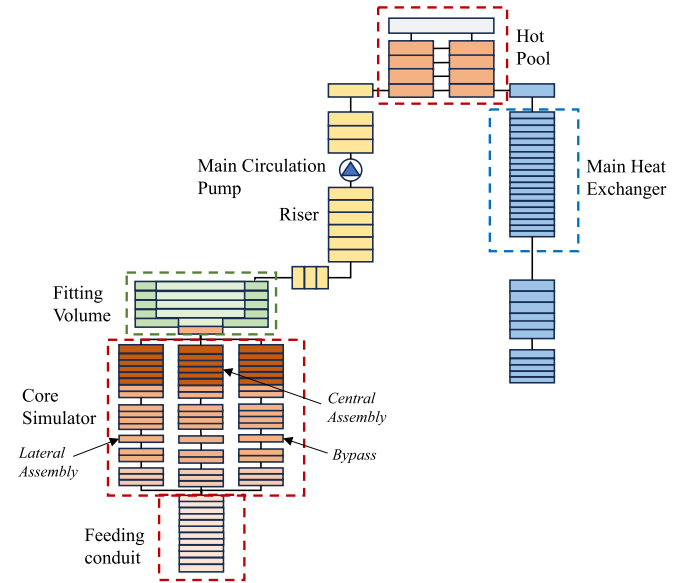**Fig. 8.** Mesh sensitivity analysis in the MHX.



**Fig. 9.** "1D" region of the primary side axial nodalization.

Fig. 10, each sector contains one of the three main primary components of the ATHENA pool: CS, MCP, and MHX.

The secondary loop (Fig. 11) has been discretized by fluid elements with a length of 15 cm in the active regions, i.e., MHX and AC, up to 25 cm in the piping sections and in the pressurizer, where the small gradients and the relatively large flow areas allow the adoption of larger axial meshes, following the general rule of maintaining a length-to-diameter ratio greater than 1 for each mesh (Information System Laboratories).

The AC air side has been modelled by a pipe component, whose boundary conditions are imposed by the inlet and outlet time dependent volumes, and a time dependent junction that fixes the mass flow rate required to obtain the required water temperature at the AC outlet.

## 4. RELAP5 results

### 4.1. Steady state results

A numerical steady state has been achieved through a 20000 s of "null transient" calculation, during which the boundary conditions outlined in Table 3 were applied. It is worth to highlight that the lead



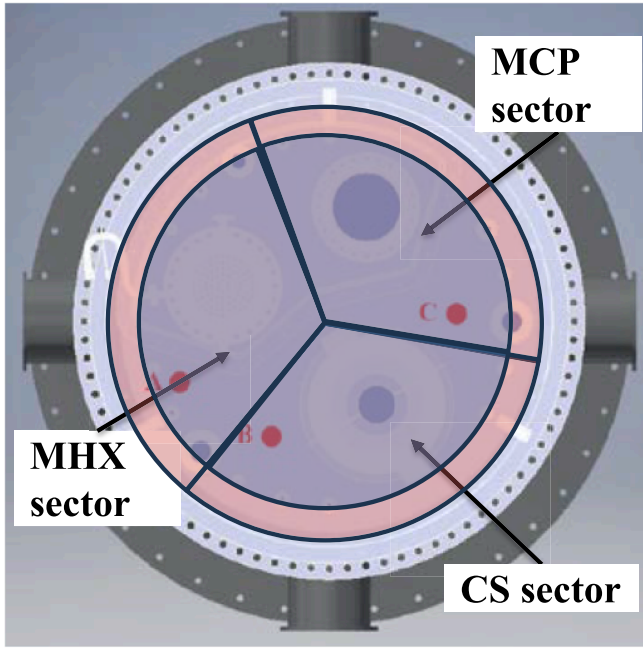**Fig. 7.** Mesh sensitivity analysis in the CS.

**Fig. 10.** Pool azimuthal nodalization.

and water mass flow rates correspond to the set point values for regulating their respective pump speed, while the air mass flow rate in the AC is regulated by a control system that adjust the air flow rate to maintain a water outlet temperature from the AC at 110 °C.

The steady state results are reported in Tables 4 and 5, along with a comparison with the design data, obtained either by CFD calculations (Cioli Puviani et al., 2023; Cioli Puviani, 2022) and detailed component calculations (Del Moro and Cioli Puviani, 2022; Del Moro et al., 2023) which have shown a general good agreement with the RELAP5 results of the entire system. The total power supplied to the lead is delivered by the CS (2210 kW) and by the MCP (7.41 kW). The power is evacuated by the system through the MHX (2200.29 kW) and the heat losses towards the environment (19.30 kW). The global energy balance deviates from zero by approximately 2 kW, which is less than 0.1 % of the CS power. Consequently, the steady state condition is considered achieved. The components from the CS to the MHX have double-wall structures, i.e.,

two metallic layers separated by an air gap, to ensure effective insulation from the cold pool, except for the curve downstream the fitting volume: due to manufacturing and installation constraints, it cannot be realized with a double wall structure. Moreover, the bottom of the hot pool is not a double wall component, resulting in significant heat losses from the hot leg towards the cold pool (38.39 kW).

The lead enters the CS at 404.2 °C with a total mass flow rate of 126.5 kg/s. It then distributes almost evenly among the central FA and the external FAs, while only 1.26 % of the total mass flow rate enters the IW region, resulting in different temperature rises in each region. The mixing temperature at the CS outlet is 522.3 °C. Then, the hot lead enters the MHX at a slightly lower temperature (520.9 °C) due to the internal heat losses, and exits the MHX at 403.8 °C.

The total pressure drops, indicating the pump head required to the MCP, amount to 89.67 kPa, mostly localized in the CS (77.81 kPa, excluding the feeding conduit). Conversely, the pressure drop in the MHX is negligible because of the significantly lower velocity compared to the CS (about 0.1 m/s and 1 m/s, respectively). The pressure drop calculated in this component are those with the highest discrepancy with the design data, but its impact on the overall pressure drop is negligible. The pressure drop from the MHX to the feeding conduit causes an increase in the level of the hot pool compared to the cold pool of about 2.6 cm, corresponding to a total pressure drop of 2.7 kPa.

Regarding the secondary side, the heat from the MHX (2200.29 kW) and the pump (6.87 kW) is dissipated by the AC (2228.49 kW) and through the heat losses towards the environment (1.94 kW). The latter are small because of the relatively low temperature of the secondary loop. Pressurized water at 2.5 MPa enters the MHX at about 110 °C, where it is pre-heated by the hot water exiting the MHX because of the

**Table 3**
Boundary conditions for the ATHENA steady state operation.

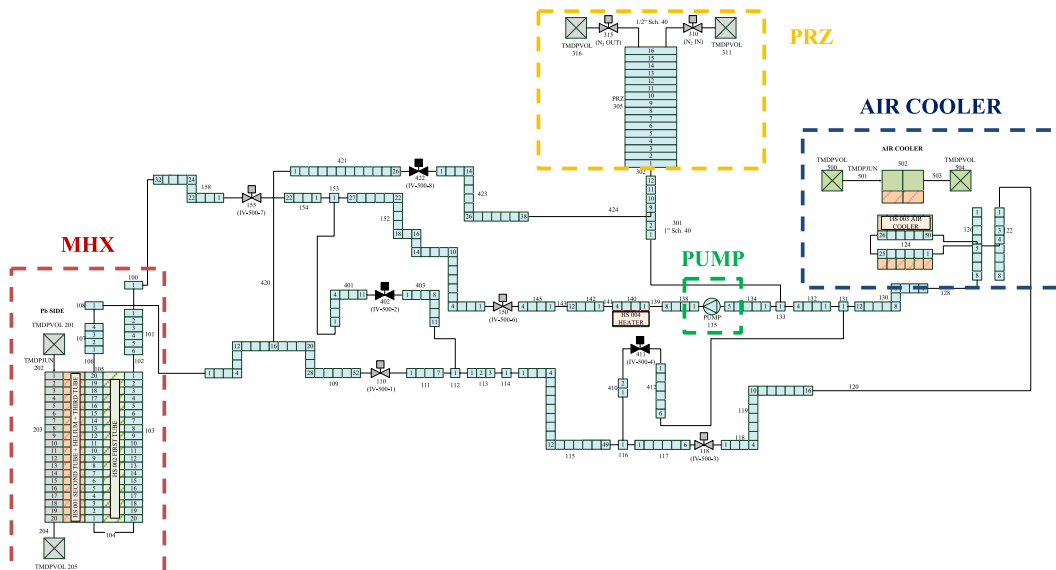| Parameter | Unit | Value |
|---|---|---|
| CS power | MW | 2.21 |
| Cover gas pressure | MPa | 0.135 |
| Cover gas temperature | °C | 400.0 |
| Pb mass flow rate set point | kg/s | 126.5 |
| Water pressure in the PRZ | MPa | 2.50 |
| Water temperature at AC outlet | °C | 110.0 |
| Water mass flow rate set point | kg/s | 7.5 |
| Environmental temperature | °C | 10 |
| Convective heat transfer coefficient with the environment | W/m$^2$ K | 8.0 |



**Fig. 11.** Secondary loop nodalization.

**Table 4**
ATHENA primary side steady state characterization.

| Parameter | Location | R5 | Design | Δ |
|---|---|---|---|---|
| Powers (kW) | CS | 2210.00 | 2210.00 | 0 % |
| | MCP | 6.37 | N/A | N/A |
| | MHX | 2200.29 | 2210.0 | −0.4 % |
| | Heat Losses | 19.30 | N/A | N/A |
| | Internal heat losses | 38.39 | N/A | N/A |
| Temperatures (°C) | CS in | 404.2 | 400.0 | 4.2 °C |
| | Ext. FAs out | 523.2 | 521.2 (Cioli Puviani et al., 2023) | 2.0 °C |
| | Cen. FA out | 521.3 | 520.5 (Cioli Puviani et al., 2023) | 0.8 °C |
| | IW out | 520.3 | 514.0 (Cioli Puviani et al., 2023) | 6.3 °C |
| | CS out | 522.3 | 520.0 °C | 2.3 °C |
| | MHX in | 520.9 | 520.0 °C | 0.9 °C |
| | MHX out | 403.8 | 400.0 °C | 3.8 °C |
| Mass flow rates (kg/s) | MCP | 126.5 | 126.5 | 0 % |
| | Ext. FAs | 64.94 | 64.52 | −0.7 % |
| | Cen. FA | 59.97 | 59.96 | 0.0 % |
| | IW | 1.59 | 2.02 | 21 % |
| Absolute pressures (MPa) | Bottom of the pool | 1.085 | N/A | N/A |
| | Cover gas | 0.135 | 0.135 | 0 % |
| Pressure drops (kPa) | CS | 77.81 | 83.16 (Cioli Puviani, 2022) | −6.4 % |
| | MHX | 0.63 | 0.42 (Del Moro and Cioli Puviani, 2022) | −50.0 % |
| | Total | 89.67 | 91.36 (Del Moro and Cioli Puviani, 2022) | −1.8 % |
| Level difference between hot and cold pool (m) | Hot and cold pool | 0.026 | N/A | N/A |

**Table 5**
ATHENA secondary side steady state characterization.

| Parameter | Location | R5 | Design | Δ |
|---|---|---|---|---|
| Powers (kW) | MHX | 2200.29 | 2210.0 | −0.4 % |
| | AC | 2228.49 | 2210.0 | 0.8 % |
| | PC | 6.87 | N/A | N/A |
| | Heat Losses | 1.94 | N/A | N/A |
| Temperatures (°C) | MHX in | 110.1 | 110 | 0.1 °C |
| | MHX riser inlet | 195.6 | N/A | N/A |
| | MHX out | 179.2 | 190.0 (Del Moro et al., 2023) | −10.8 °C |
| | AC in | 179.2 | 200.0 | −20.8 °C |
| | AC out | 110.0 | 110.0 | 0 % |
| Mass flow rate (kg/s) | PC | 7.5 | 7.5 | 0 % |
| Absolute pressures (MPa) | PRZ | 2.50 | 2.50 | 0 % |
| | MHX in | 2.72 | 2.50 | 8.8 % |
| Pressure drops (kPa) | MHX | 28.04 | N/A | N/A |
| | AC | 1.67 | N/A | N/A |
| | Total | 418.93 | 860.0* | N/A |

* it is the maximum allowable value



**Fig. 12.** Decay heat curve.

bayonet type of the heat exchanger, it enters the tube riser at 195.6 °C and exits at 179.2 °C. The mass flow rate is equal to 7.5 kg/s, leading to a total pressure drop of about 4.2 bar in the loop because of the relatively small dimension of the piping (2″) that causes velocities of the order of 3.8 m/s.

### 4.2. Transient results

#### 4.2.1. Boundary conditions

Starting from the steady state described in Section 4.1, the LOHS transient has been triggered by the closure of the MHX interception valves (SoT, Start of Transient). Therefore, the system has no more a heat sink causing an increase in the lead outlet temperature of the MHX, until the set point of 450 °C is reached and the CS is switched off following the decay heat curve shape foreseen for the ALFRED reactor, shown in Fig. 12, and applied also by other experiments simulating the ALFRED DHR (Del Moro et al., 2023; Lorusso et al., 2023). The MCP is assumed to work for the entire duration of the transient.

Since ATHENA is not equipped with a Decay Heat Removal system (DHR), the average temperature of the pool increases in the long term. This increase is limited by the thermal inertia of the pool, which is much larger than the ALFRED one: while the ratio of the volumes is 5.5 (416 m³/76 m³), the ratio of the powers is 135 (300 MW/2.21 MW), meaning that the power density of ATHENA is much lower than the ALFRED one.
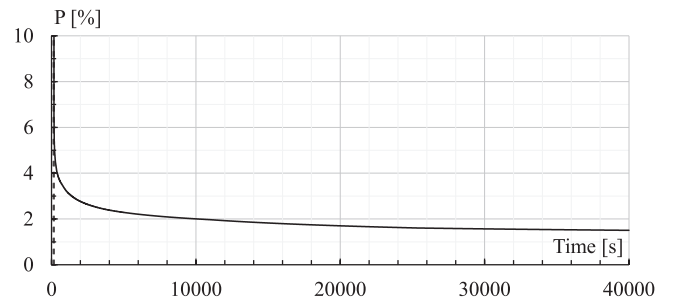
In the long term, the only heat sink consists in the heat losses towards the environment, that become of the same order of magnitude of the decay heat (see Fig. 22).

A hand calculation of the thermal inertia of the system can be performed considering only the coolant inventory in the cold pool, i.e. the lead at 400 °C in normal operation. Since the "cold" volume is about 5 m³, the energy required to increase the temperature of the pool of 1 °C is:

$$E = V_{coldpool} \bullet \rho_{Pb}(400°C) \bullet c_{p,Pb} \bullet \Delta T = 5m^3 \bullet 10580 \frac{kg}{m^3} \bullet 153 \frac{J}{kg°C} \bullet 1°C$$

$$= 8.12 MJ$$

Assuming a long term average value of the decay heat of 35 kW (∼1.5 % of the nominal power), the time needed to deliver that energy to the lead is about 230 s. It means that the average temperature of the pool should increase of about 15 °C/hour. The actual value will be even lower since this calculation does not consider the thermal inertia of the solid structures and heat losses, which at that level of power become relevant in the overall power balance. However, even in the worst-case scenario, there is still a large margin for intervention and completely switch off the CS, preventing any harming condition for the facility.

In order to consider the difference between ALFRED and ATHENA heat losses, the decay heat curve has been modified to limit the distortions due to the scaling of the facility. This operation is necessary since the heat losses are one of the parameters that are usually not scaled in

experimental facilities because of the generally low scaling factor and higher surface to volume ratio compared to the 1:1 system. For the calculation of the new decay curve, two contributions have been added according to Eq. (1): the first is the difference between the ATHENA and the "scaled" ALFRED heat losses, and the second is the difference between the thermal power provided by the MCP and the ALFRED primary pumps:

$$P_{decay,new} = P_{decay,old} + (P_{loss,ATHENA} - P_{loss,ALFRED}$$
$$\bullet f) - (P_{pump,ATHENA} - P_{pump,ALFRED} \bullet f) \tag{1}$$

Where:

- $P_{decay,new}$ is the calculated decay heat curve that has been applied for this transient;
- $P_{decay,old}$ is the scaled decay heat curve from ALFRED;
- $P_{loss,ATHENA}$ and $P_{loss,ALFRED}$ are the heat losses of ATHENA and ALFRED, respectively, evaluated at steady state;
- $P_{ATHENA}$ and $P_{ALFRED}$ are the nominal power of ATHENA and ALFRED, i.e., 2.21 and 300 MW, respectively;
- $f$ is the ATHENA to ALFRED power ratio (2.21/300 MW).

The ALFRED heat losses have been estimated assuming a cylindrical shape of the reactor vessel (8.8 m height and 8 m diameter), surrounded by 10 cm of insulator with thermal conductivity of 0.07 W/m K. This value results in about 65 kW dissipated towards the environment. The evaluation of the thermal power provided by the primary pumps in ALFRED reactor can be evaluated by the volumetric flow rate and the total pressure drop (Narcisi et al., 2020), and assuming an efficiency for the pump of 0.8. This contribution results in about 83 kW provided to the lead.

### 4.2.2. Analysis of the results

Transient simulations have been carried out with a maximum time step of $10^{-3}$ s in the first 600 s, and then relaxed up to $10^{-2}$ s, when the system approaches to a new steady state condition. As soon as the MHX is isolated from the secondary loop, the water contained in the bayonets starts to boil because of the very high temperature difference between the two fluids, and the steam is firstly vented in the PRZ, and then towards the environment, in a similar way to the shutdown procedure of the facility (Del Moro et al., 2023). Fig. 13 shows that the mass flow rate going towards the MHX is stopped in 5 s, and the MHX reaches the saturation temperature (as shown in Fig. 14) in less than 300 s, emptying completely.

Fig. 15 shows the consequent increase of the lead outlet temperature and the achievement of the set point value (450 °C) for the CS shutdown
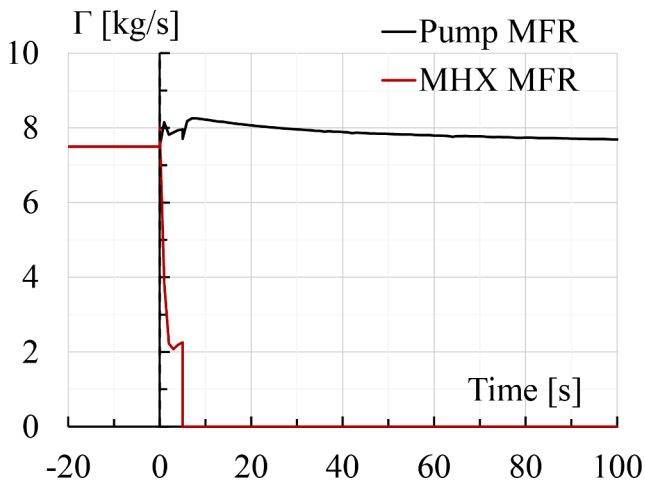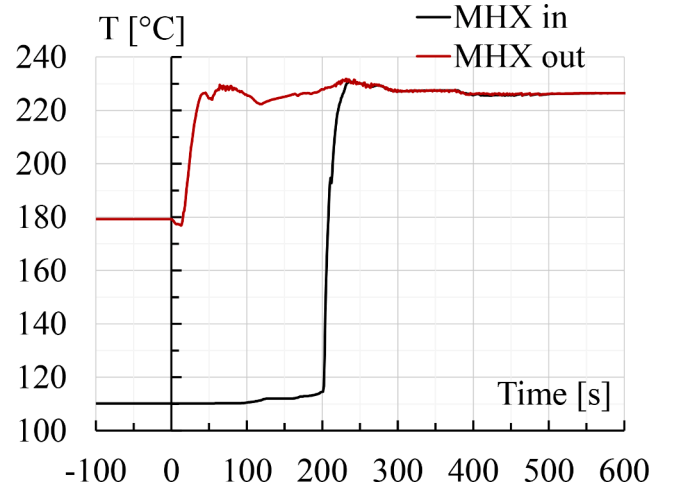


**Fig. 14.** Water temperatures at MHX inlet and outlet in the first 600 s.

at 156 s from the MHX isolation. Different time windows (TWs) during the MHX emptying before the final lead temperature decrease can be distinguished among the main events occurring in the transient and summarized in Table 6:

- TW1 0–78 s: a first increase of the lead temperature is due to the stop of the feedwater going to the MHX;
- TW2 78–112 s: the following reduction of the lead temperature is due to the efficient cooling mechanism of the boiling water in the MHX moving towards the PRZ through the MHX venting line. Boiling in the MHX can be seen observing the high heat transfer coefficient and steam quality in the secondary side between TW1 and TW2 in Fig. 17 and Fig. 18, respectively.
- TW3 112–156 s: the lead temperature increases up to set point value (450 °C) because the MHX is almost emptied and it is not able anymore to remove the nominal power;
- TW4 156–208 s: the temperature continues to increase because the effect of the colder lead plug has not yet reached the MHX;
- TW5 208–400 s: the second decrease of the lead outlet temperature (and increase of the removed power) is due to the cooling effect of the cold water remained in the feedwater collector passing through the bayonets when the valve installed at the top of the PRZ (PRZ venting valve) is opened. Fig. 19 show the valve opening ratio, which is greater than zero between TW4 and TW5, allowing also the secondary pressure to stay around the nominal value (see Fig. 20). A
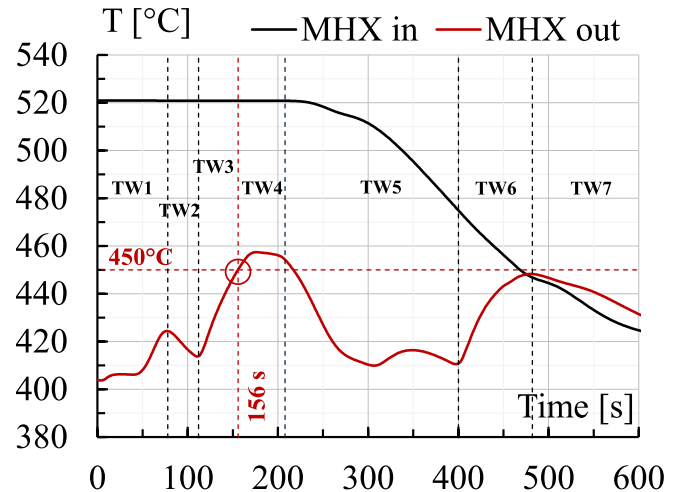


**Fig. 13.** Water mass flow rate at the pump and MHX inlet valve locations.



**Fig. 15.** Lead temperatures at MHX inlet and outlet in the first 600 s.

**Table 6**
Sequence of events during the Loss-Of-Heat-Sink transient.

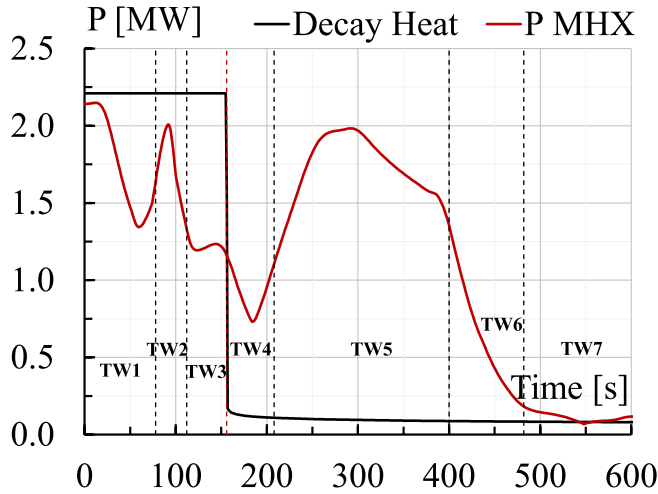| Event | Time [s] |
|---|---|
| MHX isolation | 0 |
| Water flow rate is null and start of pool boiling | 0–112 |
| Pb temperature rise and achievement of the shutdown set point | 112–156 |
| Pb temperature continues to increase | 156–208 |
| Cold water passage in the MHX due to the PRZ venting valve opening | 208–400 |
| No power exchange in the MHX | 400–482 |
| Cold lead reaches the MHX | >482 |



**Fig. 16.** Power balance in the first 600 s.
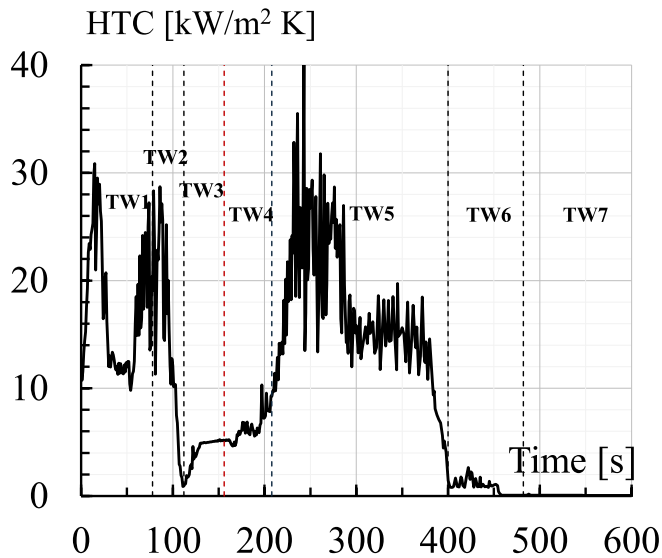


**Fig. 17.** Average heat transfer coefficient in the MHX (water side).

similar phenomenology is discussed also in Ref. (Del Moro et al., 2023);

- TW6 400–482 s: the temperature increases because the MHX is not able anymore to remove the power, and this increase is due to the hotter lead coming from the hot pool that has not been cooled.
- TW7 > 482 s: from this point on, temperature decreases because the cold lead from the CS has reached the MHX.

Fig. 16 shows the unbalance between the power provided to the lead by the CS and the power delivered to the secondary side in the short
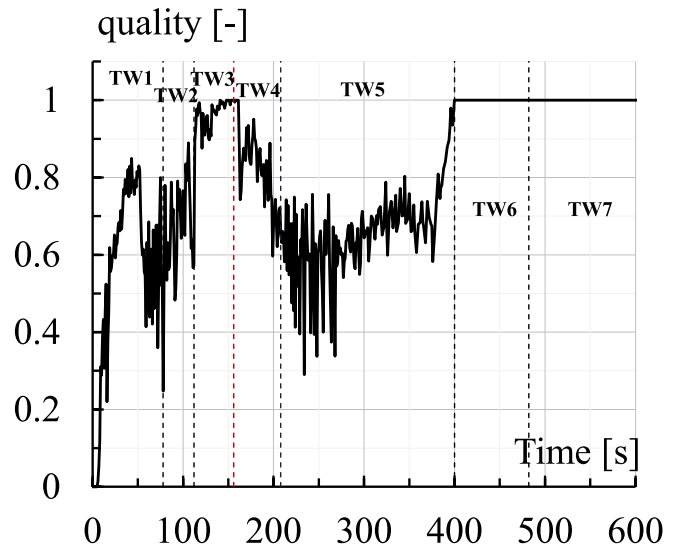


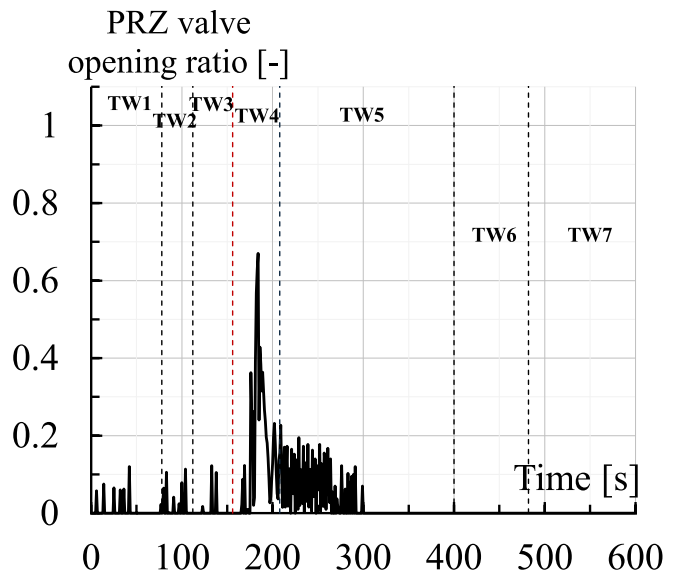**Fig. 18.** Average quality in the MHX (water side).



**Fig. 19.** Pressurizer venting valve opening ratio.

term, where it is highlighted that the power removed in the MHX is lower than the CS power, while it remains higher from the shutdown until about 500 s.

Regarding the CS temperatures, as soon as the heating element is switched off, temperatures in the active region starts to decrease because the mass flow rate is kept constant at the steady state value, therefore high temperatures are not reached in the short term nor in the long term, as shown in Figs. 21, 23 and 24. In the cold pool, the axial temperature profiles in the barrel and in the vessel regions are shown in Figs. 25 and 26, respectively. In both sides, the average temperature increase is of about 12 °C, thus potentially harming conditions for the facility are far to be reached in this transient. The reason is that the total lead inventory is much higher compared to the ALFRED one, and the unbalance between the input power compared to the removed power is compensated by the high thermal inertia of the system.

To conclude this section, the effect of the initial conditions on the LOHS transient, i.e., the conditions representative of the ALFRED Stage 2 and 3, has been evaluated. The two main effects on the transient are the following:
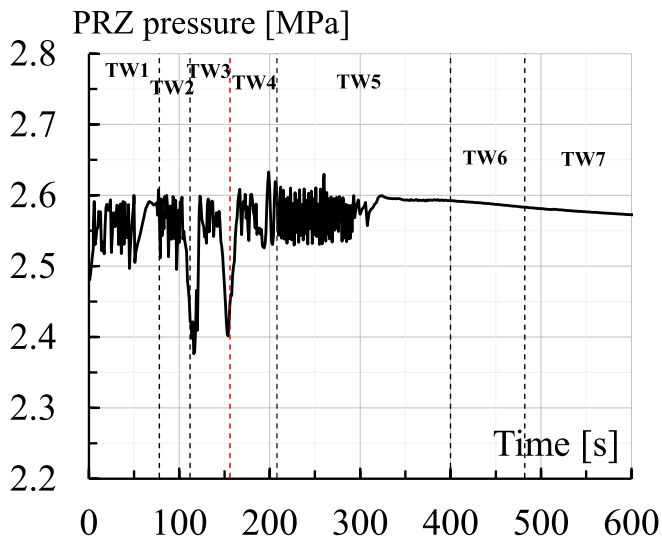
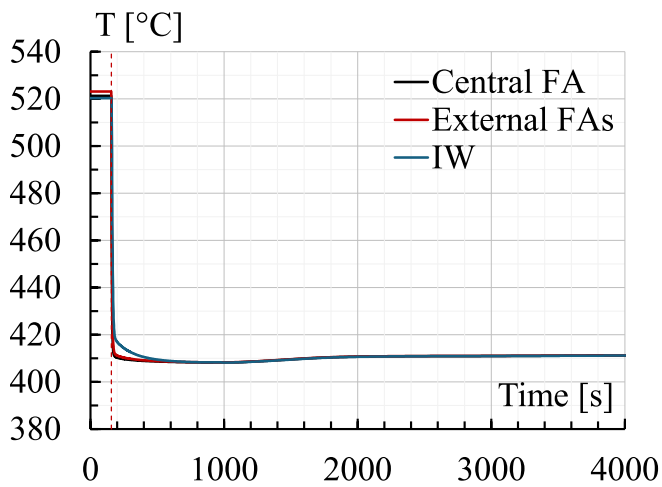**Fig. 20.** Pressure in the pressurizer.



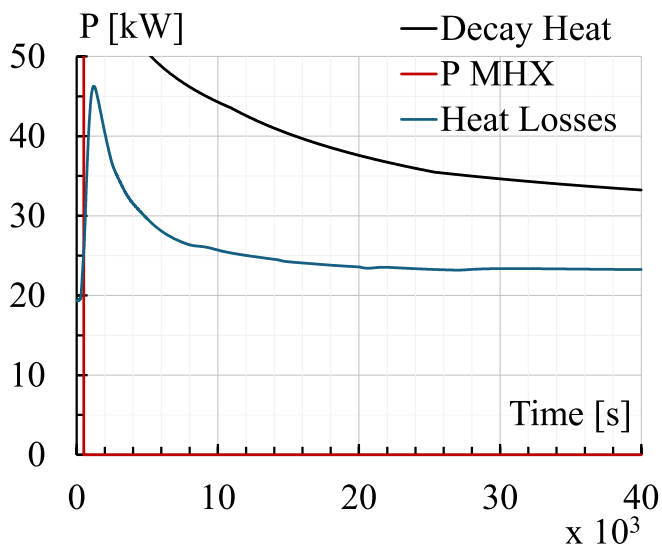**Fig. 21.** Lead temperatures at CS outlet in the first 600 s.



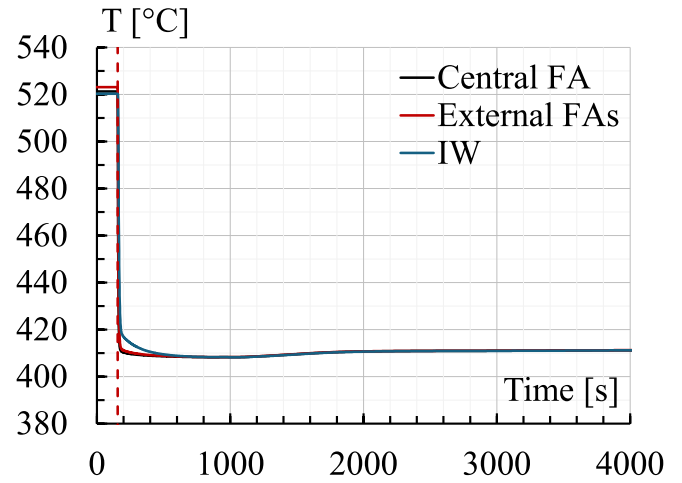**Fig. 22.** Power balance in the long term.



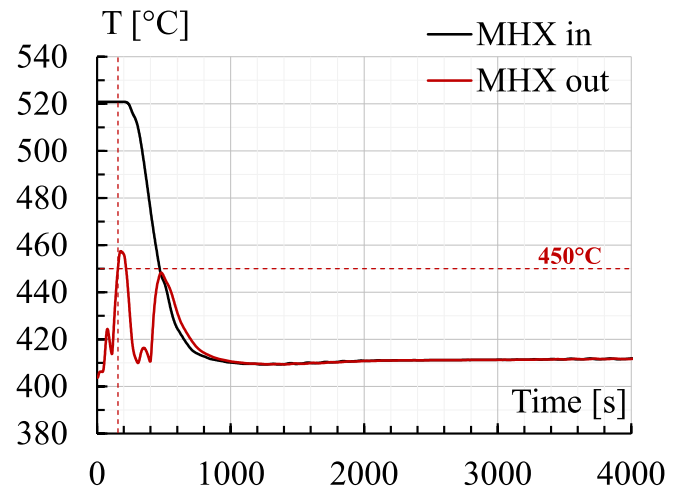**Fig. 23.** Lead temperatures at CS outlet in the long term.



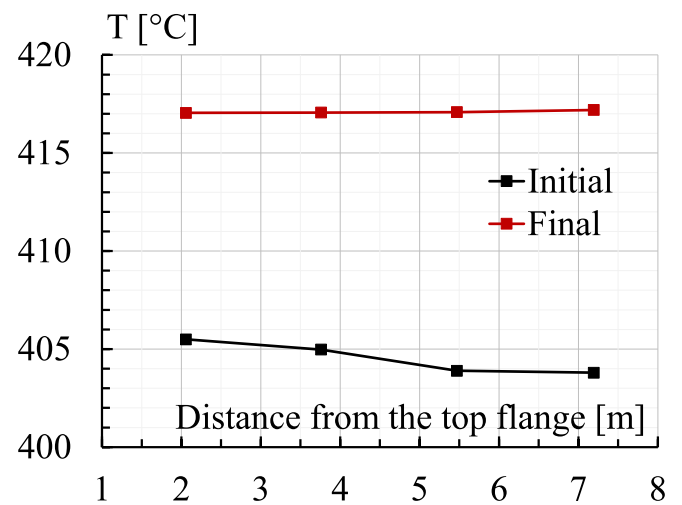**Fig. 24.** Lead temperatures at MHX inlet and outlet in the long term.



**Fig. 25.** Lead temperature profile in the barrel region before and after the transient.
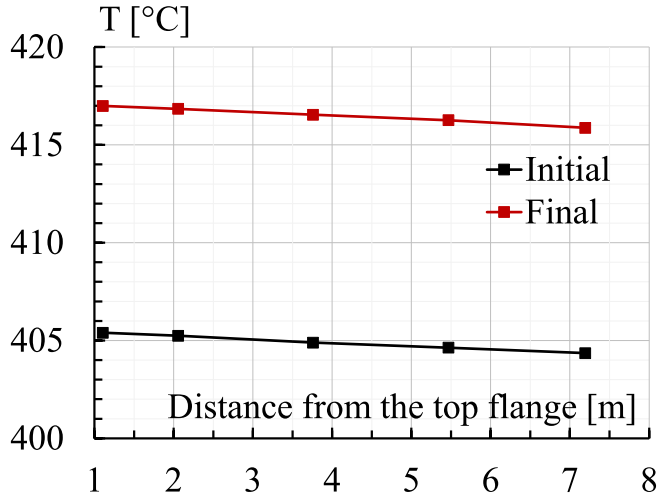
**Fig. 26.** Lead temperature profile in the vessel region before and after the transient.



**Fig. 28.** Effect of the initial conditions on the lead temperatures at MHX inlet and outlet in the long term.

- the delay in the CS shutdown (212 s vs 156 s) because more time is required for the lead in the MHX to reach 450 °C if the inlet temperature is lower (480 °C vs 520 °C). Fig. 27 shows the shift between the curves;
- the minimum temperature (red curve in Fig. 28) is lower if Stage 2 conditions are adopted for the transient. Again, this is due to the lower inlet temperature in the MHX.

In the long term, equilibrium temperature reached by the system is close to the Stage 3 initial conditions.

*4.3. Sensitivity analysis on the core simulator shutdown temperature set point*

Since the temperature rise at the MHX outlet is quite unregular because of the transition from single phase to two phase heat transfer modes at the secondary side, a sensitivity analysis on the CS shutdown signal, i.e., lead temperature set point at the exit from the MHX, has been performed. Starting from the same initial conditions, three further simulations have been carried out to assess the effect of temperature signals of 430, 470 and 490 °C. Such set points have been selected in order to investigate a sufficient number of intervention points of the shutdown system before too high temperatures are reached in the
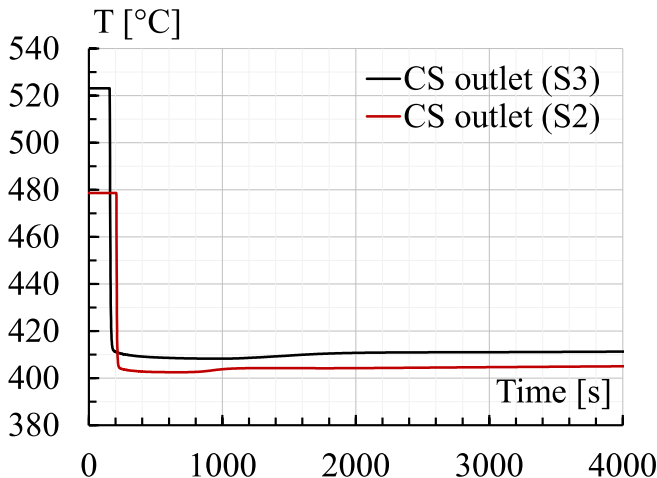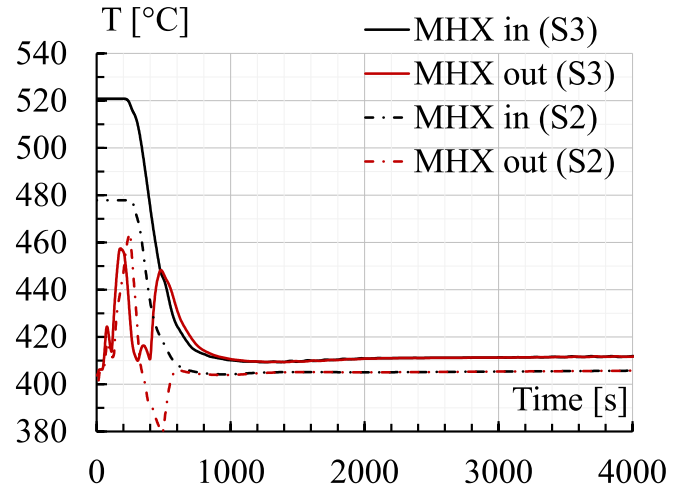
system, harming the integrity of the structures. Moreover, since the behavior of the system at the beginning of the transient is very sensitive to the shutdown time, and large oscillations characterize the MHX outlet temperature, a sensitivity on this parameter is required to assess the capability of the system to bring the facility in a safe condition despite the predicted uncertainties in the shutdown time by the numerical calculation.

In the short term, the different set points have an impact on the time of the CS shutdown: in particular, changing the set point to 430 °C leads to an anticipation of the shutdown of about 25 s (as shown in Figs. 29 and 30, where the case at 430 °C, 470 °C and 490 °C are represented in red, blue and green, respectively), with a dynamic of the system very similar to the reference case (450 °C). Instead, if the set point is moved to 470 °C or 490 °C, the shutdown is delayed of about 300 s because the efficient cooling by the MHX boiling water causes a strong temperature decrease, before rising again at about 400 s, when the MHX is almost completely emptied and not able to remove power. Therefore, moving the set point after the maximum of about 460 °C, the time required for the water to boil must be waited before the intervention of the shutdown system.

Fig. 31 show that a new quasi-steady state is achieved in the long term in all the simulations, even though the higher is the CS shutdown set point, the higher is the final equilibrium temperature. This is due to
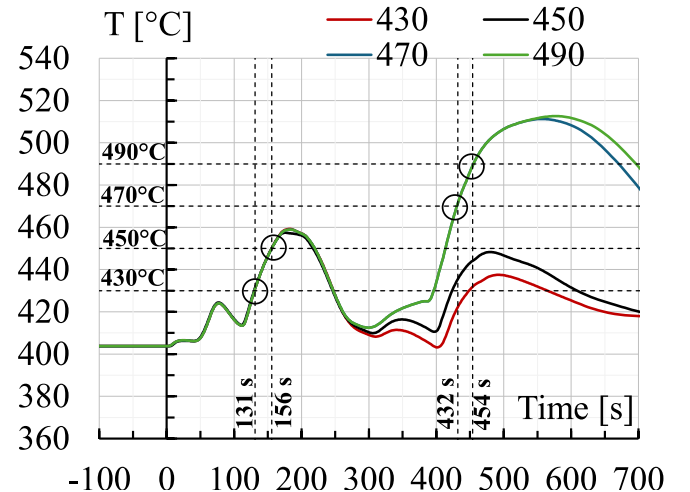


**Fig. 27.** Effect of the initial conditions on the lead temperatures at CS outlet in the long term.



**Fig. 29.** Effect of different CS shutdown temperatures on the MHX outlet temperature in the short term.
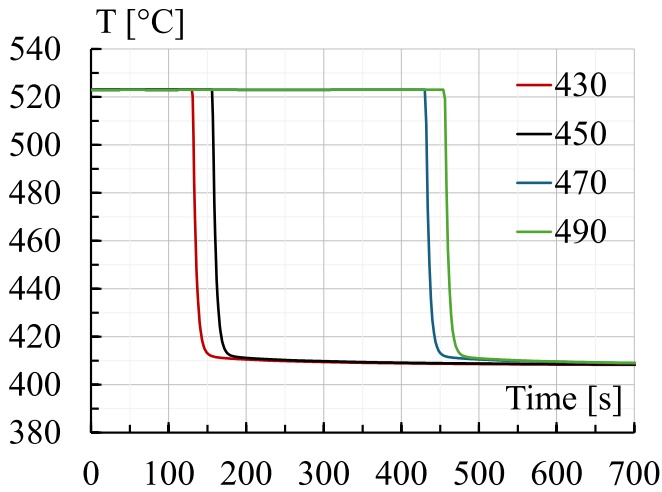
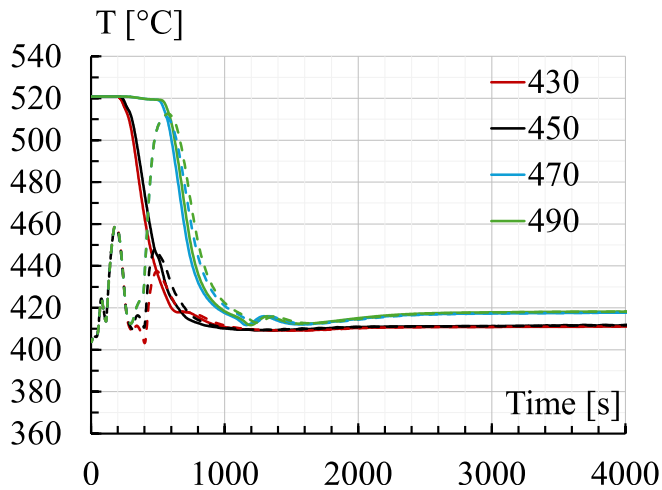**Fig. 30.** Effect of different CS shutdown temperatures in the short term.



**Fig. 31.** Effect of different CS shutdown temperatures on the MHX inlet and outlet temperatures in the long term.



**Fig. 32.** Effect of different CS shutdown temperatures on the CS outlet temperatures in the long term.
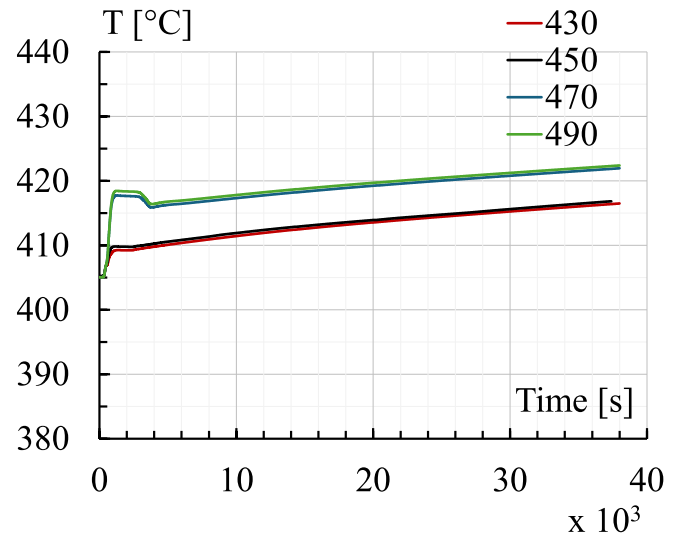


**Fig. 33.** Effect of different CS shutdown temperatures on the vessel region temperatures.

the higher amount of energy absorbed by the system before the CS shutdown. In any case, no conditions potentially harmful to the facility are reached, as shown by the temperature trend at the core outlet (Fig. 32) and in the vessel region (Fig. 33). Fig. 34 shows that the average increase of the lead temperature in the vessel region is about 17 °C, compared to the 12 °C increase for the reference case.

## 5. Conclusions

In the framework of the R&D program for the advancement of Generation IV Nuclear Power Plants, the LFRs stand out as particularly promising due to their maturity and safety features. ALFRED, serving as the European demonstrator of this technology, will be constructed in Romania, along with the related RI to investigate aspects typical of the LFRs for the physics and technology advancement, as well as for code validation. ATHENA is part of the RI and constitutes a fundamental milestone for the ALFRED R&D activities since it will be the largest pool-type facility in Europe, allowing to test components and systems in relevant scale for ALFRED reactor, and in general it will allow studies on the thermal–hydraulic aspects typical of the LFRs. In addition, it will test coolant chemistry control systems within a large pool environment.

AHTENA will be the largest lead-cooled pool type facility in Europe, featuring 3.2 m in diameter and 10 m in height. It keeps the relative height consistent with the thermal barycenters of the heat source and
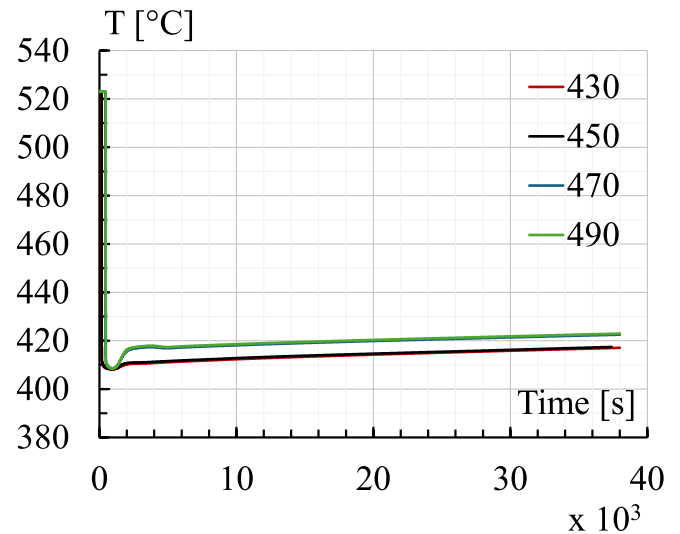
heat sink of ALFRED reactor, that is about 3.3 m. The primary and secondary systems of the facility have been described in Section 2.0, while Section 3.0 presents the numerical model developed using the system thermal–hydraulic code RELAP5/Mod3.3.

The boundary conditions defining the operational parameters of the facility have been presented in Section 4.1, and the numerical steady state has been obtained accordingly by the code. Then, the Loss-Of-Heat-Sink (LOHS) transient has been analyzed. The LOHS is initiated by the closure of the MHX isolation valves, causing a temperature rise of the lead at the MHX outlet. At 164 s from the SoT, the temperature reaches the set point of 450 °C, triggering the shutdown of the CS. Consequently, the power reduces to 7 % of the steady state value, gradually decreasing according to the decay heat curve.

The numerical analysis evidenced that the temperature rise in the pool is not significant due to the very high thermal inertia of ATHENA compared to the ALFRED reactor, allowing to absorb substantial power variations without posing any risk to the facility. In the long term, the heat losses from the main vessel towards the environment effectively mitigate temperature increases in the primary system. This is evident in
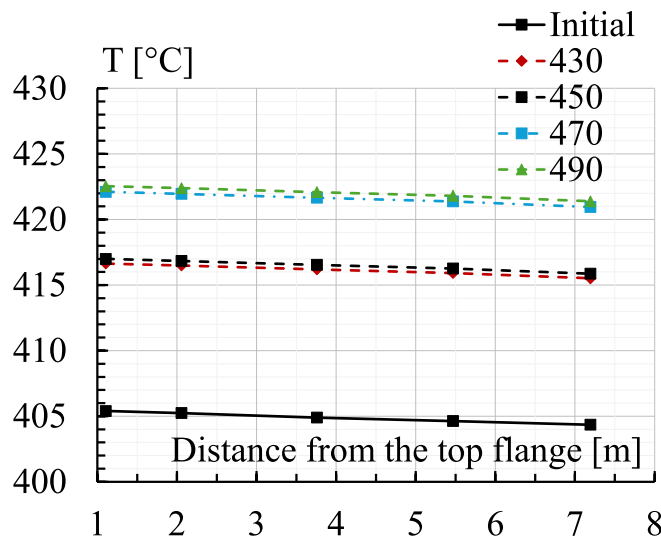
**Fig. 34.** Effect of different CS shutdown temperatures on the final temperature profile along the vessel.

the modest 12 °C increase observed in the temperature of the cold pool, both in the barrel and the vessel regions.

A numerical sensitivity analysis on the temperature set point for the CS shutdown has been carried out to assess the behavior of the system if the set point is moved to 430, 470 and 490 °C. It has been shown that the lower is the set point, the lower is the temperature at the MHX outlet. On the contrary, if the set point is moved to 490 °C, the CS shutdown is delayed of about 300 s, causing a greater energy deposit in the lead before the shutdown. Therefore, a higher final equilibrium temperature is achieved in the system, i.e., 17 °C rise of the temperature in the vessel region.

The results presented in this paper can be considered as a pre-test simulation, and they have shown the feasibility of the experiment, confirming the lack of any risk for the facility. Moreover, they will be compared with the experimental data to assess the performances of the RELAP5 code in simulating large pool systems with lead as a working fluid.

**Declaration of competing interest**

No potential conflict of interest was reported by the author(s).

**Data availability**

The data that has been used is confidential.

**References**

Alemberti, A. et al. (2015). "ALFRED and the Lead Technology Research Infrastructure," in *Proceedings of the International Topical Meeting on European Research Reactor Fuel Management (RRFM)*, Bucharest, Romania.

Cioli Puviani, P., Di Piazza, I., Marinari, R., Zanino, R., Tarantino, M., 2023. Multiscale thermal-hydraulic analysis of the ATHENA core simulator. Nucl. Technol. 210 (4), 692–712.

Cioli Puviani, P. (2022). "ATHENA Core Simulator. Thermo-Fluid Dynamic Design," ENEA Report AT-N-R-597.

Constantin, M., Grasso, G., Tarantino, M., Turcu, I., Paunoiu, C., Toma, A., Caramello, M., Frignani, M., Alemberti, A., Diaconu, D., Nitoi, M., Apostol, M., Gugiu, D., Agostini, P., 2021. The development of the research infrastructure in support of ALFRED demonstrator implementation in Romania. EMERG - Energy Environ. Effic Resour. Global. VII (1), 123–132.

Del Moro, T., Cioli Puviani, P. (2022). "ATHENA Main Flow Path Analysis," ENEA Report AT-D-R-621.

Del Moro, T., Lorusso, P., Giannetti, F., Tarantino, M., Caramello, M., Vitale Di Maio, D. (2022). "ATHENA Main Heat Exchanger Conceptual Design and Thermal-Hydraulic Assessment with RELAP5 Code," in *Proceedings of the 2022 29th International Conference on Nuclear Engineering (ICONE29)*, Shenzhen, China.

Del Moro, T., Giannetti, F., Khalil Youssef, G., Lorusso, P., Caramello, M., Cauzzi, M.T., Tarantino, M. (2023). "Post-Test Analysis of SIRIO Facility Data by System Thermal-Hydraulic Codes for LFR Application," in *Proceedings of the 20th International Topical meeting on Nuclear Reactor Thermal Hydraulics (NURETH-20)*, Washington, D.C.

Del Moro, T., Lorusso, P., Giannetti, F., Tarantino, M., Caramello, M., Mazzi, D., Constantin, M., 2023. ATHENA main heat exchanger conceptual design and thermal-hydraulic assessment with RELAP5 code. J. Nucl. Eng. Radiat. Sci. 9.

Del Moro, T., Giannetti, F., Tarantino, M., Lorusso, P., Caramello, M., Vitale Di Maio, D., Constantin, M., 2023. Thermal-hydraulic characterization and numerical modeling with RELAP5 code of ATHENA secondary loop. Nucl. Technol. 210 (4), 591–607.

Frignani, M., Alemberti, A., Tarantino, M., 2019. ALFRED: a revised concept to improve pool related thermal-hydraulics. Nucl. Eng. Des. 335 (15).

Frignani, M., Alemberti, A., Villabruna, G., Adinolfi, R., Tarantino, M., Grasso, G., Pizzuto, A., Turcu, I., Valeca, S. (2017). ALFRED: A Strategic Vision for LFR Deployment," in *Transactions of the American Nuclear Society*, Washington, D.C.

Gen IV International Forum, "Generation IV Goals," [Online]. Available: https://www.gen-4.org/gif/jcms/c_9502/generation-iv-goals.

Grasso, G., Petrovich, C., Mattioli, D., Artioli, C., Sciora, P., Gugiu, D., Bandini, G., Bubelis, E., Mikityuk, K., 2014. The core design of ALFRED, a demonstrator for the European lead-cooled reactors. Nucl. Eng. Des. 278, 287–301.

Information System Laboratories, RELAP5/Mod3.3 Code Manual Volume V: User's Guidelines.

Information System Laboratories, "RELAP5/Mod3.3 Code Manual Volume I: Code Structure," 2003.

Lorusso, P., Bassini, S., Del Nevo, A., Di Piazza, I., Giannetti, F., Tarantino, M., Utili, M., 2018. GEN-IV LFR development: status & perspectives. Prog. Nucl. Energy 105, 318–331.

Lorusso, P., Tarantino, M., Nitti, F.S., Achilli, A., Cauzzi, M.T., Caramello, M., Hamidouche, T., Fernandez, R., Rozzia, D., Kljenak, I., Krpan, R., Jimenez, G., Queral, C., Del Moro, T. (2023). "Numerical Analysis and Code Qualification Based on SIRIO Experiments Within the PIACE Project," in *Proceedings of the 20th International Topical Meeting on Nuclear Reactor Thermal Hydraulics (NURETH-20)*, Washington, D.C.

Martelli, E., Giannetti, F., Ciurluini, C., Caruso, G., 2019. Thermal hydraulic modeling and analyses of the water cooled EU DEMO using RELAP5 system code. Fusion Eng. Des. 146 (Part A), 1121–1125.

Narcisi, V., Giannetti, F., Caruso, G., 2019. Investigation on RELAP5-3D© capability to predict thermal stratification in liquid metal pool-type system and comparison with experimental data. Nucl. Eng Des. 352.

Narcisi, V., Giannetti, F., Caramello, M., Caruso, G., 2020. Preliminary evaluation of ALFRED revised concept under station blackout. Nucl. Eng. Des. 364, 110648.

Oriolo, F., et al., 2000. Modifiche del Codice RELAP5 versione MOD3.2 per la Simulazione di Sistemi Refrigerati con leghe di Pb o Pb-Bi. University of Pisa.

Tarantino, M., et al., 2021. Overview on lead-cooled fast reactor design and related technologies development in ENEA. Energies 14 (16).